

Design and Performance of an Open loop Controlled Reciprocating Reluctance Motor

M. E. Abdel- Karim, A. H. Morsi

*Dept. of Elect. Eng., Faculty of Eng.
Minufiya University, Shebin El- Kom, EGYPT.*

Abstract--- This paper describes the design and performance of an open loop controlled reciprocating reluctance motor, fed from a single-phase ac voltage controller. The controller is implemented using power transistor switches depends on PWM concept. The motor consists of moving iron bar inside a coil connected in series with a capacitor. The motor operates on the basis of resonance in an RLC stator circuit. The ac transistor voltage controller is employed to match the characteristics of the proposed reciprocating motor, whereas it has a variable power factor angle during one cycle of motor stroke. With this controller, the motor voltage can be smoothly controlled from zero to full supply voltage, to avoid the variation of capacitor in a stepwise fashion. Consequently, the amplitude of force and motor stroke can be varied smoothly by varying the duty cycle of the power transistor switches. Also, a proposed design of the coil parameters of the motor is introduced according to the desired motor driving force and its stroke. The theoretical analysis and computed performance of the system with different supply conditions are confirmed by experimental results of a laboratory prototype.

1. Introduction

A linear travelling electromagnetic field is produced in a manner analogous to that in ac machines, can be utilized to produce reciprocating motion. The operation of reciprocating motor can be understood by imagining a conventional cylindrical machine cut open and laid flat, in which a unidirectional force is produced. Continuously reciprocating motion can be obtained by an arrangement of two half windings [1-3], arranged back to back, each of them produces an electromagnetic wave traveling linearly in opposite direction to the other. Other design refers to the first linear electric motor invented in 1838, and also to the oscillating motor discussed by Blakley[2], and Mendrela[1]. It consists of a coil with an iron bar moving inside it. This type

Manuscript received from Dr. A.H. Morsi on : 11 / 8/1999

Accepted on : 6/11/1999

Engineering Research Bulletin, Vol 23, No 1, 2000 Minufiya University, Faculty of Engineering , Shebien El-Kom , Egypt, ISSN 1110-1180

of motor operation may be used to operate a pile driver, electric hammer, and spinning industry. However, the previous researches did not give design of the motor dimensions. An external capacitor was used in the previous motor designs to enable the reciprocating motor operates on the basis of resonance state in an RLC circuit. At the resonance positions, the driving current increases sharply and consequently the driving force will be increased. This current depends mainly on the value of the applied voltage in one side. In the other side, the motor current also depends on the resonance positions which occurs according to the value of capacitor which resonates the RLC circuit motor. However, varying the value of motor capacitor in stepwise fashion can not give a smooth variation of the motor speed and driving force.

In this paper, a single-phase ac voltage controller is used to obtain the motor voltage which can be smoothly controlled from zero to full supply voltage. Normally, the considered reciprocating motor changes its character from a capacitive to inductive mode, i.e. has a variable power factor angle, during one cycle of the motor stroke. So, employing an ac thyristor voltage controller technique gives a variable motor voltage waveforms, even when the firing angle is fixed. Also, the motor voltage contains harmonics at multiples of supply voltage frequency which becomes excessive, if discontinuous conduction occurs. Besides, the slow response of the ac thyristor voltage controller is due to its inherent dead time lag[4-6].

In this paper, to overcome the above problems of this technique, an ac voltage controller employing power transistors which operate in PWM concept is designed. This controller can be smoothly control the motor voltage from zero to the full supply voltage. The ac transistor voltage controller has inherently fast response. The high-frequency ripple at the motor current is easily filtered by the nature of RLC motor circuit. Also, a proposed design of the coil parameters of the motor such as number of coil turns, coil inductance, coil resistance are introduced. This design depends on the desired motor driving force and its stroke.

2. Principle of Operation

The proposed reciprocating reluctance motor with an open loop control circuit is shown in Fig.1a. It consists of a coil with a Ferro-magnetic bar moving inside it. The coil is connected in series with a capacitor and fed from a single phase ac transistor voltage controller and operates in PWM concept. The inductance L of the coil varies according to the bar position. The capacitor is used for tuning the circuit to resonance state when the end of the bar comes close to any coil edge. The bar in this position is pulled back into the coil due to a strong magnetic field generated by a heavy resonant current. Because of its inertia, the bar passes by the coil center and tends to move towards the other end of the coil. Again, a resonance occurs in this position, causing a

heavy current to flow in the coil. Then, the bar is stopped and starts to move back towards the other coil end and so on. This movement is possible because the magnetic force which drives the bar towards the center of the coil is always greater than the magnetic force which brakes the bar when it moves from the center of the coil to any coil edges.

The design of the proposed motor mainly depends on the magnetic force f_m which may be expressed as [1]:

$$f_m = 0.5i^2 \frac{dL}{dx} \quad (1)$$

This force depends on the square of the motor current i and the rate of the coil inductance variation due to the bar movements x . At the resonance positions, this force is the desired motor force and is named the driving force while the magnetic force which brakes the bar at the center of the coil is named braking force. The driving current, depends mainly on the value of the motor voltage and the resonance positions. So, an ac transistor voltage controller depends on PWM concept, as shown in Fig.1, is used to obtain the motor voltage which can be smoothly controlled from zero to full supply voltage. Consequently, the amplitude of driving force and motor stroke can be controlled.

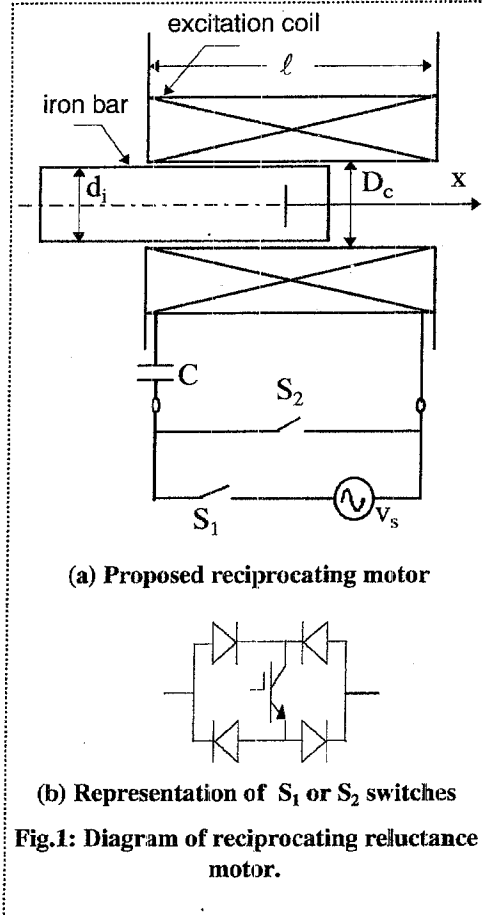


Fig.1: Diagram of reciprocating reluctance motor.

3. Design Objectives and Procedures

3-1. Coil inductance

Traditionally, in machine design the dimensions are obtained for specific power, power factor and speed. For the proposed motor, however, the objectives are to obtain the proper coil design for a specific dimensions, to calculate the coil inductance which ensures the required force and stroke length. To achieve these objectives, the dimensions shown in Fig. 1a is considered to obtain the coil inductance as follows. As related to Fig.1a, in steady state, the inductance of any coil can be obtained from[7]:

$$L = \frac{\mu N^2 A}{l} = N^2 \frac{1}{\mathfrak{R}_{eq}} \quad (2)$$

where: N no. of coil turns,
 A cross section area,
 ℓ length of coil, which is equal to the length of bar,
 μ permeability of core,
 \mathfrak{R}_{eq} equivalent magnetic reluctance of core.

The equivalent magnetic reluctance can be represented by three reluctances \mathfrak{R}_1 , \mathfrak{R}_2 , and \mathfrak{R}_3 connected as shown in Fig.2, where:

$$\mathfrak{R}_1 = \frac{x}{\mu_0 A_1}, \quad \mathfrak{R}_2 = \frac{x}{\mu_r A_i}, \quad \text{and} \quad \mathfrak{R}_3 = \frac{\ell - x}{\mu_0 A_3},$$

where: $A_1 = \frac{\pi}{4}[D_c^2 - d_i^2]$, $A_i = \frac{\pi}{4}d_i^2$, and $A_3 = \frac{\pi}{4}D_c^2$.

μ_r is the relative permeability of the iron bar which is manufactured from iron with B-H curve, as shown in Fig.3. From the principle of operation of the proposed motor, the length of the coil ℓ can be taken as half length of the desired motor stroke of one coil side.

Then,
$$\mathfrak{R}_{eq} = \mathfrak{R}_3 + \frac{\mathfrak{R}_1 \mathfrak{R}_2}{\mathfrak{R}_1 + \mathfrak{R}_2}$$

$$= \frac{\ell - x}{\mu_0 A_3} + \frac{x(\ell - x) / \mu_0 \mu_r A_1 A_i}{(x / A_1) + (\ell - x) / \mu_r A_i} \quad (3)$$

The variation of coil inductance with bar position at different numbers of coil turns is obtained by solving (2) and (3) where, the other coil dimensions are considered constant. The inductance of the saturated bar, which most likely occur actually when the bar is around the center of the coil, nearly have a fixed value as shown from the measured curve in Fig.4. While, the calculated curves of coil inductance, from (2), increase significantly when the bar moves near the center of the coil, i.e x nearly is zero. So, these curves are fitted to give the theoretical results shown in Fig.4, to match the measured curve.

From Fig.4, it is noticed that with a low number of coil turns, dL/dx has a different values and sometimes zero near the coil edges. While, for high number of coil turns, dL/dx has a nearly zero value for a wide region

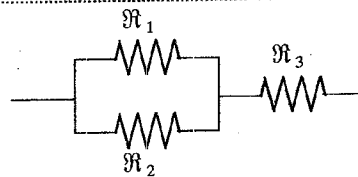


Fig.2: The equivalent magnetic reluctance of proposed motor.

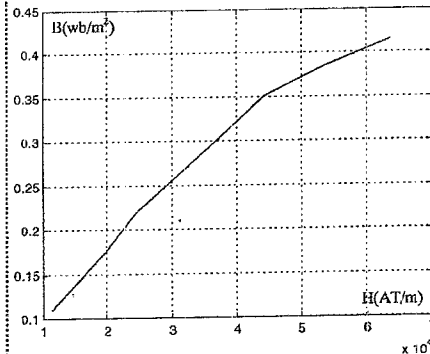


Fig.3: Measured B- H curve for iron bar of motor.

around the coil center. In between, dL/dx has a nearly constant value for a wide region of both coil edges. So, this leads to choose N to be 4500 turns, which gave a nearly constant value of dL/dx in both coil edges as required in (1).

The characteristic of the coil inductance of Fig.4 can be determined from the deduced empirical expression:

$$L = K\left(\frac{x}{\ell}\right)^4 - 1.3 * K\left(\frac{x}{\ell}\right)^2 + L_{\max} \quad (4)$$

where: $K = L_{\max} + L_{\min}$
 L_{\min} inductance of the coil without the bar, and
 L_{\max} inductance of the coil with the bar placed at the center of the coil, i.e at $x=0$.

For the chosen coil turns (N is 4500 turns), the corresponding dL/dx can be determined from Fig.4 at the end of coil, and consequently the driving current (maximum current), can be calculated from (1) according to the required driving force.

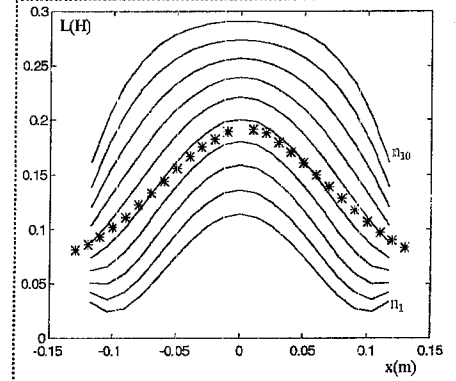


Fig.4: The variation of coil inductance with the position of bar at different number of coil turns:
— theoretical curves at N_1 (500 turns) to N_{10} (15000 turns),
** measured curve at $N=4500$.

3. 2- Coil resistance

The chosen coil turns N is divided by the number of layers N_v and the number of turns per layer N_h as:

$$N = N_v * N_h \quad (5)$$

The diameter of coil without insulation, d_b , is obtained from:

$$d_b = \sqrt{\frac{4I}{\pi J}} \quad (6)$$

where:

J current density (J for copper $=5A/mm^2$, has been taken),
 I maximum current.

The number of turns per layer is calculated, taking into account the diameter with insulation (d) as:

$$N_h = \frac{\ell}{d}; \quad N_v = \frac{N}{N_h} \quad (7)$$

Then, the copper depth, $d_c = dN_v$, and the mean length of the coil turn ℓ_t is:

$$\ell_t = \pi(D_c + d_c) \quad (8)$$

Therefore; the coil resistance can be obtained as:

$$R = \frac{\rho \ell_i N}{a} \quad (9)$$

where: a cross sectional area of coil = $\pi d_b^2 / 4$.

4. Control Circuit

The control circuit is designed to adjust the switching operation of the electronic switches to suit the gate requirements as it will be discussed. The motor coil is fed by the ac voltage controller using power transistor switches S_1 and S_2 which depends on the PWM concept[4-5], as shown in Fig.1a. These switches are IGBT's of type "25Q101" and used to control the motor voltage smoothly from zero to the full supply voltage. In order to operate in either directions, each switch is fed through a fast recovery diode bridge as shown in Fig.1b. The ac transistor switches which connected in series and in shunt are controlled so that any power factor angles can be satisfactory handled. Therefore, the switches operate simultaneously. When S_1 is turned on and S_2 is turned off, the motor is fed from the supply voltage. When the switch S_2 is turned on and the switch S_1 is turned off, a freewheeling current is passed through S_2 , while the supply voltage is disconnected by S_1 .

- PWM and steering circuit

The drive transistor circuit receives a train of pulses from the PWM and steering circuit as shown in Fig.5. The comparator compares a triangle signal of switching frequency with a dc reference voltage V_{ref} . Its output is fed to the drive circuit through a NAND latch circuit. Such circuit ensures that, S_1 is turned off just when S_2 is on. Each switch operates at a switching frequency of 1 KHz much higher than the supply frequency of 50 Hz. However, the duty cycle of the transistor switches determines the motor voltage level and accordingly the desired motor speed. The motor voltage increases due to increasing the duty cycle of S_1 by increasing V_{ref} . The switching frequency can be considered relatively high, so, a fast recovery diodes are then required.

5. Mathematical Model

The electromechanical system of the reciprocating motor, shown in Fig.1, can be simulated by two non-linear second-order differential equations. The first one represents the electrical equation:

$$\begin{aligned} \frac{d(L * i)}{dt} + R i + \frac{1}{C} \int i dt &= v_s \quad \text{if } S_1 \text{ on and } S_2 \text{ off} \\ \frac{d(L * i)}{dt} + R i + \frac{1}{C} \int i dt &= 0 \quad \text{if } S_1 \text{ off and } S_2 \text{ on} \end{aligned} \quad (10)$$

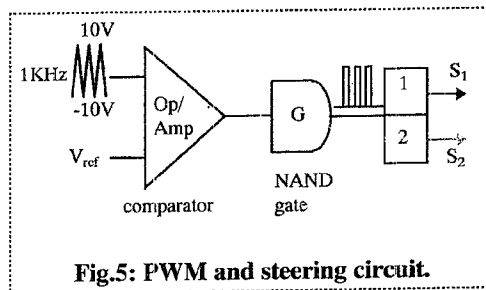


Fig.5: PWM and steering circuit.

and the second one represents the mechanical equation:

$$m \frac{d^2 x}{dt^2} + f_r \frac{dx}{dt} = f_m \quad (11)$$

where: L coil inductance,
 i instantaneous motor current,
 v_s motor voltage = $V_{sm} \sin(\omega t)$,
 m mass of the bar,
 f_r damping coefficient which represents the bar's friction,
 f_m magnetic force acting upon the bar, found by (1).

Both sides of (10) should be differentiated with respect to time, to avoid the integration problem. Consequently, eqns (1, 10 and 11) may be rewritten in a suitable form for numerical calculations as:

$$\begin{aligned} \ddot{x} &= (0.5L_d \dot{i}^2 - f_r \dot{x}) / m \\ \dot{i} &= \left\{ \omega V_{sm} \cos(\omega t) - [R + 2L_d \dot{x}] \dot{i} - \left[\frac{1}{C} + L_{dd} (\dot{x})^2 + L_d \ddot{x} \right] i \right\} / L \\ &\quad \text{for } S_1 \text{ on and } S_2 \text{ off,} \\ &= \left\{ -[R + 2L_d \dot{x}] \dot{i} - \left[\frac{1}{C} + L_{dd} (\dot{x})^2 + L_d \ddot{x} \right] i \right\} / L \\ &\quad \text{for } S_1 \text{ off and } S_2 \text{ on} \quad (12) \end{aligned}$$

where: $L_d = \frac{\partial L}{\partial x}$, and $L_{dd} = \frac{\partial^2 L}{\partial x^2}$ and can be calculated from eqn (4).

The electromechanical eqn. (12) will be written in state-space form, to solve it using Simulink MATLAB software as follows:

$$\begin{aligned} \dot{y}_1 &= y_2, \\ \dot{y}_2 &= (0.5L_d y_3^2 - f_r y_2) / m, \\ \dot{y}_3 &= y_4 \quad \text{and,} \\ \dot{y}_4 &= \left\{ \omega V_{sm} \cos(\omega t) - [R + 2L_d y_2] y_4 \right. \\ &\quad \left. - \left[\frac{1}{C} + L_{dd} y_2^2 + L_d (0.5L_d y_3^2 - f_r y_2) / m \right] \right\} / L \\ &\quad \text{for } S_1 \text{ on and } S_2 \text{ off, and} \\ &= \left\{ -[R + 2L_d y_2] y_4 - \left[\frac{1}{C} + L_{dd} y_2^2 + L_d (0.5L_d y_3^2 - f_r y_2) / m \right] \right\} / L \\ &\quad \text{for } S_1 \text{ off and } S_2 \text{ on} \quad (13) \end{aligned}$$

The state variables are defined as: $x = y_1$, $\dot{x} = y_2$, $i = y_3$, $\dot{i} = y_4$.

6. Operation Considerations

6- 1. Motor voltage

If a sinusoidally alternating voltage is suddenly applied to a resonant series RLC circuit in which the inductance is due to iron cored and of low resistance exhibit a phenomenon called Ferro-resonance. This phenomenon is principally attributable to the saturation of the iron-cored inductance in the circuit as it will be explained.

The inductance of coil L depends on the relative permeability of the bar and varies with its position. This permeability depends on the magnetic flux density in the bar which changes with the voltage across the coil and the position of the bar. When the bar is moved near the center of the coil, saturation is most likely to occur. The inductance of the saturated bar decreases significantly, and this result in a high motor current in positions around the center of the coil as shown in Fig.6 which lead to increase monolithically in the motor driving force. Consequently, the motor does not operate properly in such situations. These results are taken for the supply voltage of 200 volt. To avoid this undesirable effect, the supply voltage should be kept below a voltage which causes saturation in the bar as shown from the results throughout this paper , where the base supply voltage, i.e. the duty cycle is 100 %, is taken at 165 volt.

6-2. Motor capacitor

Normally, the value of capacitor will be chosen to tune the circuit to resonate at the end of coil edges depends on the following relation:

$$\omega_0^2 = 1/LC \quad (14)$$

where ω_0 is the resonant frequency $= 2\pi f$,

For a certain position of the measured coil inductance, shown in Fig.4, which determine the desired motor stroke, the required capacitor will be calculated by (14). Accordingly, and from the test results, a capacitor value of 75 μF was found to be suitable for the full range of the desired driving force and duty cycle variations. With this value of the capacitor, the bar moves with fixed oscillations around the center of the coil. But, for a capacitance higher than 75 μF , the circuit will be tuned at two positions of the bar in one side of the coil. Consequently the bar moves with fixed oscillations in one side of the coil. This reduces the motor stroke as shown in Fig.7 and consequently the motor force. Also, when the capacitance is much lower than 75 μF , the circuit will be tuned to resonant at two positions of the bar around the center of the coil nearly close to each other. This yields a driving force always less than the braking force and consequently the motor then fails to start.

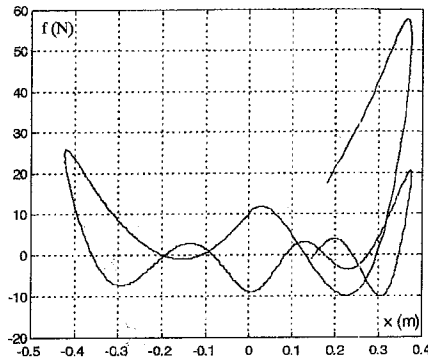


Fig.6: The force of the motor versus the bar's position with undesirable Ferro-resonance phenomenon due to $V_s = 200\text{V}$, $C = 75\mu\text{F}$, and $V_{ref} = 10\text{V}$.

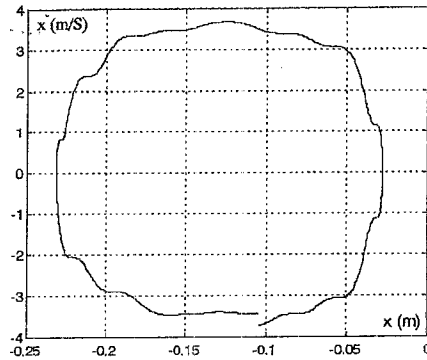


Fig.7: The speed of the motor, moves in one side of the coil, versus the bar's position due to $C = 2 \times 75\mu\text{F}$, $V_s = 160\text{V}$, and $V_{ref} = 10\text{V}$.

7. Simulated Results

Simulated results are obtained to predict the motor performance under various output forces and at different supply conditions such as variations of the motor voltages via the variations of the duty cycle and/or at different supply frequencies. Also, the simulated results provide important insights into the motor behavior, and subsequently are useful in designing the final construction of the motor and the laboratory procedure.

To obtain the motor performance characteristics under the proposed technique of control, eqns (1,4, and 13) listed above, which describe the whole operation of the system, were solved with the aid of a personal computer using Simulink Matlab software. These characteristics are obtained for the following motor dimensions:

- length of the coil,	$\ell = 0.15 \text{ m}$,
- mass of the bar,	$m = 0.4 \text{ Kg}$,
- diameter of the bar,	$D_c = 0.019 \text{ m}$,
- resistance of the coil,	$R = 11.5 \Omega$,
- damping coefficient,	$f_r = 1.4 \text{ N-s/m}$,
- number of coil turns,	$N = 4500 \text{ turns}$,
- frequency of supply voltage	$f = 50 \text{ Hz}$.

The coil parameters of the simulated motor are calculated from eqns. (2-9). The bar is considered free to move through the coil, i.e without mechanical stops in either edges. Alternatively, the motor stroke is not limited, and will be determined by the driving force according to the operating point.

At starting, when the motor switched on, the bar was positioned at a certain distance from the center of the coil (e.g. $x = 0.05 \text{ m}$). The bar starts to operate with stable oscillations immediately after the switch is closed. Figures 8a and 8b show the waveforms of the motor voltage and current for reference voltage

of 8 volt and the switching frequency for S_1 and S_2 is 1 KHz. However, the bar trajectory on $x - x^\circ$ plane is shown in Fig.8c.

A set of simulated results were obtained when the motor is energised by a sinusoidal voltage of 165 volt, 50 Hz and a base capacitor of 75 μ F. Figures 9, 10, and 11, show the simulated force, current, and speed of the motor at different duty cycles corresponding to a reference voltages of 1.5, 2, and 10 volt respectively. Several interesting observations obtained from these curves.

For reference voltage greater than 1.5 volt to maximum reference voltage of 10 volt, as shown in Fig.9 and Fig.10, the bar moves with stable oscillations around the center of the coil. This is because the circuit will resonate at two symmetrical positions of the bar around the center of the coil. The magnitude of the driving current and driving force are increased sharply and then diminish as the reference voltage is further increased. In Fig.9 and Fig.10, when the reference voltage is varied from 2 to 10 volt., the driving current is changed from 11 to 13 amp with driving forces of 225 and 350N respectively. The corresponding motor speed varies from 4 to 8 m/s and the motor stroke of one coil side varies from 0.3 to 0.35 m. Also, the magnitude of braking current and the corresponding braking force are inversely varied with the reference voltage level. Accordingly, the higher reference voltage, i.e., the higher the duty cycle of S_1 , the higher each of driving current, driving force, motor speed, motor stroke and lower braking force.

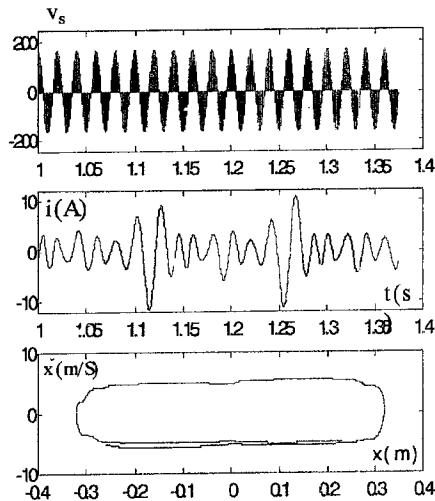


Fig.8: Simulated characteristics of the motor operating in horizontal position
 $V_s=160V$, $V_{ref}=8V$, $C=75\mu F$.

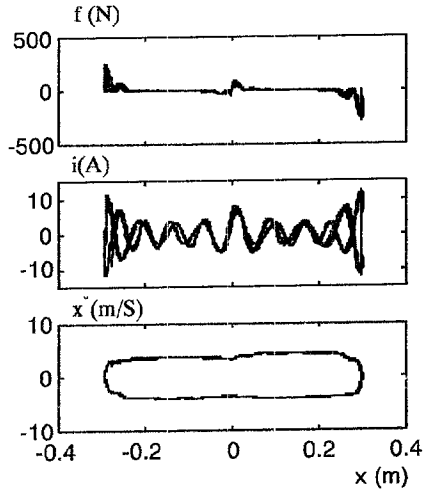


Fig.9: Theoretical characteristics of the motor with $V_{ref}=2V$, $V_s=160V$, $C=75\mu F$.

The effect of reference voltage less than 2 volt, remains the same except that the circuit will resonant at two positions of the bar in one side of the coil. Consequently, the bar moves with stable oscillation in one side of the coil as shown in Fig.11. At certain value of reference voltage, near the minimum, the force on the bar is zero everywhere.

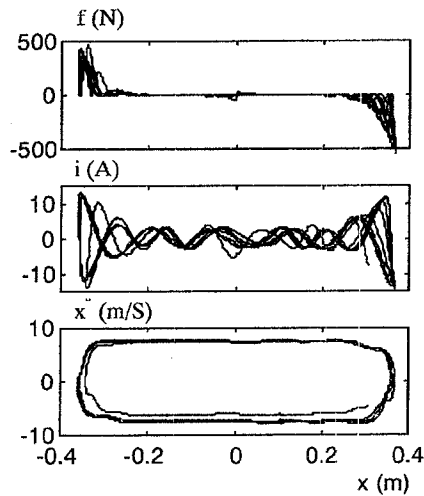


Fig.10: Theoretical characteristics of the motor with $V_{ref}=10V$, $V_s=160V$, $C=75\mu F$.

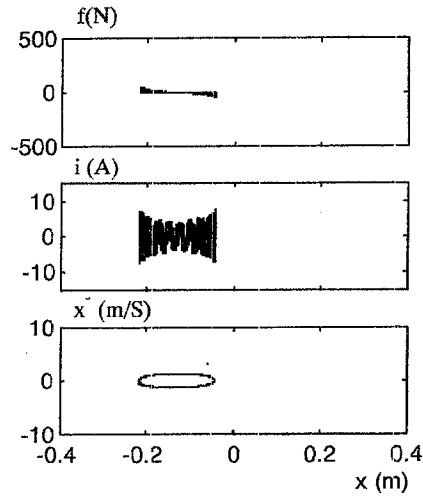


Fig.11: Theoretical characteristics of the motor with $V_{ref}=1.5V$, $V_s=160V$, $C=75\mu F$.

The previous results show the motor performance with the variation of reference i.e. the variation of supply voltage at 50 Hz. Figure 12 shows the motor performance at a reference voltage of 5 volt and the frequency of the supply voltage, f , is varied from 50 to 70 Hz. The circuit is resonated at two positions of the bar around the center at 50 Hz. Increasing of the supply frequency to 70Hz makes the circuit to resonant at two positions of the bar in one side of the coil reducing the driving force and consequently the motor stroke. Besides, the motor current remains nearly as the current at the resonance points during the complete cycle of the motor stroke. In contrast, decreasing the supply frequency from 50 to 30 Hz, the circuit remains resonant at two points around the center as well as the driving force is nearly remains as at 50 Hz, 225N, and the braking force is decreased as shown in Fig.13. Consequently, the motor stroke of one coil side is increased from 0.35 to 0.45 m and the driving current is decreased from 11 to 8 amps when the frequency is varied from 50 to 30 Hz respectively.

8. Experimental Investigations

The motor parameters which mentioned in section 7, are used to build the prototype motor. In this prototype, the motor stroke is limited by a stopping ring on the forward traverse at 1.5 of the coil length, l , from the coil center, and another symmetrical ring on the backward traverse. The motor dynamic performance is carried out at different cases, these include changing the applied voltage and the duty cycle of S_1 and S_2 . A shunt resistor of 0.05 volt/10 amp is inserted in series with the motor circuit to indicate the waveform of the motor current. The damping coefficient and coil resistance were determined experimentally as 1.5 N-s/m and 11.5 Ω respectively.

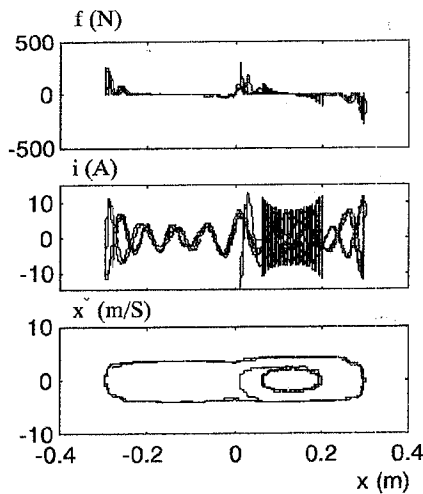


Fig. 12:Theoretical characteristics of the motor with f varies from 50 to 70Hz, $V_s=160V$, $V_{ref}=5V$, $C=75\mu F$.

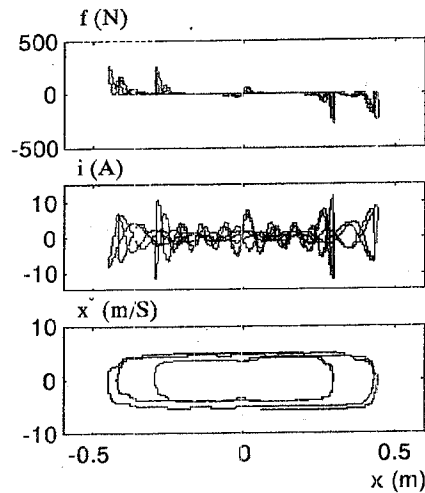


Fig.13: Theoretical characteristics of the motor with f varies from 50 to 30Hz, $V_s=160V$, $V_{ref}=5V$, $C=75\mu F$.

Figure 14 shows the oscillograms of the motor voltage and current at a supply voltage of 165 volt, V_{ref} is 10 volt, and base capacitor is 75 μF . The motor current is a modulated sinusoidal wave with a motor stroke frequency. It is noticed that the bar moves with stable oscillations around the center of the coil and the cycle of motor stroke is about 0.175 second. These results were taken for conditions similar to those assumed for simulated results (see results of Fig.8). Generally, there are no significant differences between the simulated and experimental results. Discrepancies are mainly due to the inaccurate measurement of the damping coefficient f_r . This coefficient was measured at one speed and was assumed to be constant, whereas, it may vary with the speed and the position of the bar.

Figure 15 shows the waveforms of voltage and current for the motor when operated at supply voltage of 110 volt, V_{ref} of 10volt, i.e. the duty cycle of 100 %, and the base capacitor of 75 μF . It can be seen that, when the bar is driven by the maximum driving force at resonance points, i.e at the driving current, where there is no phase shift between current and voltage, hence, the motor operates with a unity power factor. When the bar moves within the region of the coil's center, the current lags the voltage. It means that the motor changes its character from resistive and sometimes capacitive to the inductive mode. Figure 16 shows the motor voltage and current oscillograms at different duty cycles corresponding to the reference voltages of 5 and 8 volt and switching frequency of S_1 and S_2 is 1 KHz. The motor energised from a sinusoidal voltage of 165 volt, 50 Hz, and a base capacitor of 75 μF . It is noticed that the bar moves with stable oscillations around the center of the coil, which give a symmetrically driving current and consequently the driving force as shown in Fig.16. Also, the driving current is increased from 8 to 10 amp, and

consequently the driving force is increased as expected from (1). Besides, the cycle time of motor stroke is increased from 0.175 to 0.2 second as the reference voltage is increased from 5 to 8 volt respectively. This means that the motor stroke is increased as the reference voltage is further increased.

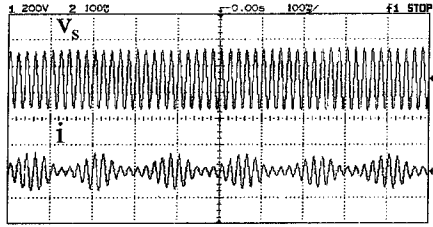


Fig.14: Experimental characteristics of the motor with $V_s=165V, V_{ref}=10V, C=75\mu F$: v_s (200V/div), i (20A/div), and time (100ms/div).

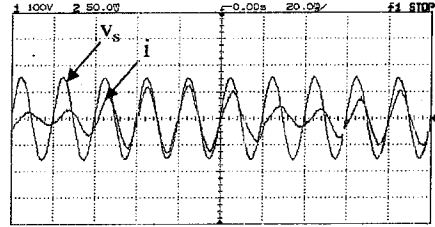


Fig.15: Experimental characteristics of the motor for one-half cycle with $V_s=165V, V_{ref}=10V, C=75\mu F$: v_s (100v/div), 10A/div, and time (20ms/div).

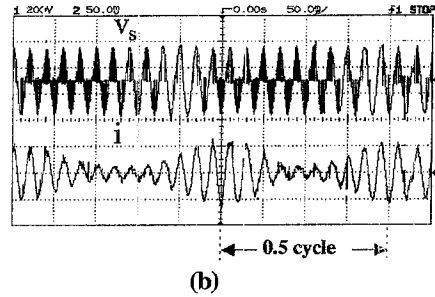
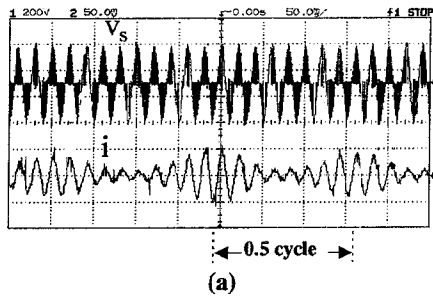


Fig.16: Experimental characteristics of the motor with $V_s=165V$, switching frequency= 1KHz, $C=75\mu F$: a) $V_{ref}=5V$, b) $V_{ref}=8V$: (v_s (200V/div), i (10A/div), and time-scale (50ms/div).

Because the switching frequency is much higher than that of the supply voltage, the capacitor voltage is nearly sinusoidal. However, apart from the small high frequency ripples, the motor current is sinusoidal due to the inductive nature of the motor. At the same reference voltage of 5 volt (duty cycle is 75 %), the motor operates under two values of switching frequency, they are 1KHz and 0.5 KHz, as shown in Fig.17a and Fig.17b

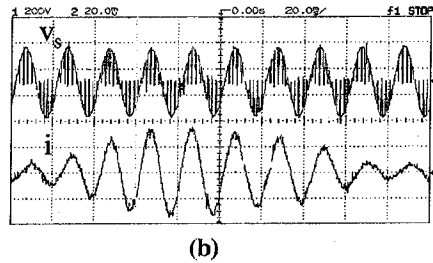
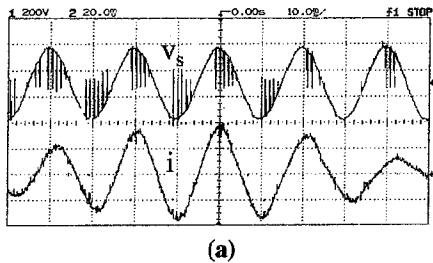


Fig.17: Experimental characteristics of the motor with $V_s=165V, V_{ref}=5V, C=75\mu F$, and switching frequency is: a) 1KHz, b) 0.5KHz: v_s (200V/div), i (5A/div), and time (50ms/div).

respectively. It is noticed that, the distortion of the motor voltage, due to the operation of switching, is increased as the switching frequency is further decreased. While, there is no significant differences in the small high frequencies ripples due to the switching frequencies on the motor currents.

9. Conclusions

The reciprocating reluctance motor control circuit is developed using single-phase ac voltage controller employing power transistor switches which operate in PWM concept. The motor operates on the basis of an electric resonance which occurs in an RLC motor circuit. Systematic method for designing the motor dimensions is introduced according to the desired motor driving force and its stroke. With the ac voltage controller, the motor voltage can be smoothly controlled from zero to full supply voltage. Accordingly, the higher motor voltage, i.e., the higher the duty cycle, the higher each of driving current, driving force, motor speed, motor stroke, and lower braking force. To operate the motor with stable oscillations around the center of the coil, the applied voltage should be kept below the voltage value which causes saturation in the bar. Also, it is necessary to use the suitable value of motor capacitor which is tuned the RLC circuit and yields driving force is always greater than the braking force. Then, the duty cycle of the transistor switches determines the motor voltage level, under the saturation voltage, and accordingly the desired deriving force and its stroke. The motor can be operate with stable oscillation in one side of the coil either by decreasing the duty cycle or increasing the supply frequency and/or the value of the motor capacitor. Experimental tests are found in a good agreement with the simulated results.

References

- 1] E. A. Mendrela, and Z. J. Pudlowski, "Transients and dynamics in a linear reluctance self-oscillating motor," IEEE trans. Energy conversion, vol. 7, no. 1, March 1992.
- 2] Blakley, "A linear oscillating ferro-resonant machine," IEEE Transactions on Magnetics, vol. MAG-19, No.4, July 1983, pp.1574-1579.
- 3] Y. C. West, and B. V. Jayawant, "A new linear oscillating motor," Proc. of IEE, 109(A), pp. 293- 300, 1962.
- 4] JR. A. Mozdzer, and B. K. Bose, "Three-phase ac power control using power transistors," IEEE Trans. Ind. Appl., vol. IA-12, pp. 499-505, Sept./Oct. 1976.
- 5] B. K. Bose, "Power electronics and ac drives," Prentice- Hall, 1986. (Book)
- 6] S. Lesan, M. Smiai, and W. shepherd, "Control of wound rotor induction motor using thyristor in the secondary circuits," IEEE Trans. Ind. Applicat., vol. 32, No. 2, March/April 1996.
- 7] A.H. Morsi, "Analysis of the solid rotor induction motor using the concept of wave impedance," MSc Thesis, Menoufiya University, 1979.
- 8] M. Abdel-Karim, and A. I. Taalab, "A single phase series active power filter for harmonic compensation of nonlinear loads," Engg. Research Bull., faculty of Engg., Menoufiya University, vol. 19, no. 3, 1996.

تصميم و دراسة أداء محرك ممانعة ترددي محكوم بدائرة مفتوحة

د/ مصطفى السيد عبد الكريم د/ أحمد حسنين مرسي

كلية الهندسة بشبين الكوم - جامعة المنوفية

ملخص البحث

قدم البحث تصميماً لمحرك ممانعة ذو حركة خطية ترددية مغذى من مصدر جهد محكوم أحادي الوجه. يتركب المحرك من قلب حديدي أسطواني الشكل يتحرك داخل ملف متصل بالتوالي مع مكثف. تعتمد حركة المحرك على الرنين بين المكثف و محاثه الملف و الذي يحدث عند أوضاع مختلفة للقلب الحديدي نتيجة تغير ممانعة الملف عند هذه المواضع. و قد تم تصميم أبعاد الملف و اختيار قيمة المكثف بحيث يعطي المحرك أكبر قوة دفع و أطول مشوار ممكن. تم التحكم في جهد المحرك باستخدام قنطرة مفاتيح الكترونية تعمل بأسلوب تعديل عرض النبضة (PWM). و باستخدام قيمة المكثف التي تم اختيارها و بتغيير حالات التوصيل و القطع للمفاتيح الالكترونية، أمكن تغيير جهد المحرك تدريجياً و بدقة من الصفر إلى القيمة المقننة لملاشاة استخدام قيم عديدة للسعة للحصول على قيم مختلفة لقوة الدفع و مشوار المحرك.

تم استنتاج نموذج رياضي غير خطي لدراسة خصائص و أداء هذا المحرك عند حالات مختلفة لتوصيل المفاتيح الالكترونية مع قيم مختلفة من سعة المكثف و تردد منبع الجهد. كذلك تم استخدام هذا النموذج لدراسة اتزان المحرك و حدود جهد المنبع التي تسبب التشبع المغناطيسي و كذلك قيم المكثف اللازمة لتوليد قوة دفع أكبر من القوة العكسية.

تم بناء و اختبار نموذج معلمي لهذا المحرك و استعرضت النتائج التي تبين خصائص التصميم المقترح عند قيم مختلفة لجهد المنبع و لسرعة توصيل و قطع المفاتيح الالكترونية، و قد تبين أن هذه القيم تؤثر على قوة الدفع و على طول مشوار المحرك. و تبين وجود تطابق جيد بين النتائج المعملية و التحليلية.